ISSN 0021-3640, JETP Letters, 2024, Vol. 119, No. 7, pp. 495–500. © The Author(s), 2024. This article is an open access publication.
Russian Text © The Author(s), 2024, published in Pis'ma v Zhurnal Eksperimental'noi i Teoreticheskoi Fiziki, 2024, Vol. 119, No. 7, pp. 492–497.

OPTICS
AND LASER PHYSICS

"Anomalous" Photoelectric Effect in the Ultrafast Electron Diffraction Method

S. A. Aseyev[a], B. N. Mironov[a], D. G. Poydashev[a,*], A. A. Ischenko[b], and E. A. Ryabov[a]

[a] *Institute of Spectroscopy, Russian Academy of Sciences, Troitsk, Moscow, 108840 Russia*

[b] *Lomonosov Institute of Fine Chemical Technology, Russian Technological University, Moscow, 119571 Russia*

**e-mail: poydashev@isan.troitsk.ru*

Received March 6, 2024; revised March 6, 2024; accepted March 7, 2024

Electron-pulse probing of fast laser-induced processes has allowed the direct observation of the structural dynamics in matter with a high spatiotemporal resolution. A thin gold film has appeared to be a convenient photocathode, and photoelectron emission has been induced by femtosecond ultraviolet radiation with a photon energy of about 4.65–4.75 eV (in particular, $\hbar\omega \cong 4.65$ eV for the third harmonic of the Ti:sapphire laser). For the linear photoelectric effect, this energy contradicts the reference work function $W_{Au} \cong 5.1$–5.3 eV of pure metal. Reasons for such contradiction have been analyzed and good agreement with experimental data has been reached with a model proposed for the generation of photoelectron pulses.

DOI: 10.1134/S0021364024600745

1. INTRODUCTION

The ultrafast electron diffraction (UED) method is widely used in current world practice covering physics, chemistry, biophysics, and nanotechnologies [1–4]. Based on the femtosecond laser technique, this method allows the detection of the laser-induced structural dynamics in matter with a high spatiotemporal resolution. This makes it possible to directly observe the coherent dynamics of nuclei (femtosecond time resolution) and electrons (attosecond time resolution) involved in photoinduced processes in free molecules and condensed matter. Unlike a large X-ray free electron laser, the UED method ensures studies with a laboratory device.

The ultrafast electron diffraction method schematically involves two channels: the laser excitation (pumping) of the sample and its probing by time-delayed electron pulses. An optical delay line allows one to represent the studied dynamics in the form of a sequence of electron diffraction patterns recorded on a position-sensitive detector in a controlled time sequence. The precise synchronization of both channels is reached due to a common master source of ultrashort laser pulses. To generate electron bunches, it is convenient to use the photoelectric effect in a metal or a semiconductor [5, 6].

The use of a semitransparent gold film as a photocathode ensured the generation of a pulsed electron beam by a quite simple and efficient transmission method. To activate such a cathode, pulsed laser radiation in the ultraviolet band (linear photoelectric effect) or in the visible band with the wavelength $\lambda \cong 560$ nm (two-photon electron emission) can be used.

The third harmonic ($\lambda \cong 265$ nm) of a femtosecond Ti:sapphire laser, which is widely used in numerous laboratories studying fast processes, appeared to be a convenient source of ultraviolet pulses. However, there is an apparent contradiction: the photon energy of this ultraviolet radiation is noticeably lower than the work function W_{Au} of pure gold presented in many reference books. Although all UED experiments were carried out in high (often ultrahigh) vacuum with thin films prepared by different methods and in different laboratories, the difference between reference values and the "actual" work function W_{Au} is noticeable and can reach about 1 eV.

The aim of this work is to reveal reasons for this discrepancy. We analyze possible reasons for a decrease in the work function of a thin-film gold cathode and indicate the factors affecting UED experiments. A model of the formation of ultrashort electron pulses is proposed to explain experimental results.

2. EXPERIMENTAL ULTRAFAST ELECTRON DIFFRACTION SCHEMES WITH THE THIN-FILM GOLD CATHODE

A high time resolution of the UED method is due to the use of ultrashort synchronized optical and electron pulses. Commercially available sources of femtosecond laser pulses with a duration reaching ≈5 fs can be used in the pump channel, whereas known difficulties appear for the probe channel (see, e.g., [1, 3, 4]).

First, the Coulomb repulsion between electrons significantly worsens the time resolution of the UED method. To reduce this effect, it is necessary to use probe bunches (with the initial transverse size of 10–30 μm determined by the diameter of the laser beam in the focal spot) containing a comparatively small, up to $\sim 10^4$, number of electrons in each pulse, to increase their kinetic energy, and to reduce the distance between the cathode and the sample. At a large acquisition time, when contributions from many pulses should be summed for the reliable detection of the electron diffraction pattern, the observation of the structural dynamics during several hours requires the stable long-term operation of the photoelectron source.

The most important features of the femtosecond electronograph distinguishing it from the large X-ray free electron laser are the comparable simplicity and compactness. To generate the pulsed electron beam in the UED method, semitransparent thin-film (several tens of nanometers) metal cathodes appeared to be very efficient because they allow the delivery of transmitting laser radiation directly to the photoelectron emission region in vacuum. The third harmonic of the femtosecond Ti:sapphire laser ($\lambda \cong 265$ nm, $\hbar\omega \cong 4.65$ eV) made it possible to implement the linear photoelectric effect in gold and silver films. Although silver ensures a higher quantum efficiency, its operation time in practice is much shorter than that of gold.

For this reason, the thin-film gold photocathode remains the basis for the elegant scheme of the formation of ultrashort photoelectron pulses in the compact UED facility (see Fig. 1) [7–14].

Using the UED method, the authors of [7] studied the photoinduced response in a high-quality silicon single crystal. It was demonstrated that the photostimulated heating of the crystal lattice can lead to a surprising increase in the intensity of Bragg peaks in the diffraction pattern, which contradicts the known Debye–Waller effect. It was shown that this behavior can be explained only in the dynamic diffraction theory including the multiple scattering of probing electrons in the sample. It was concluded that the inclusion of such effects opens a way to the quantitative study of the nonequilibrium dynamics of defects in high-quality perfect single crystals.

We note that the thin-film gold cathode was used in the setup described in [11, 12], where the fourth harmonic of a femtosecond Yb:KGW laser ($\lambda \cong 260$ nm, $\hbar\omega \cong 4.78$ eV) induced photoelectron emission in ultrahigh vacuum. The authors of [12] studied the gigahertz structural resonance in a 16-nm antiferromagnetic $FePS_3$ film cooled below the Néel temperature. The shift of layers in the sample, where individual regions of the antiferromagnetic thin film are shifted in parallel to each other as coherent oscillators, was detected by the UED method.

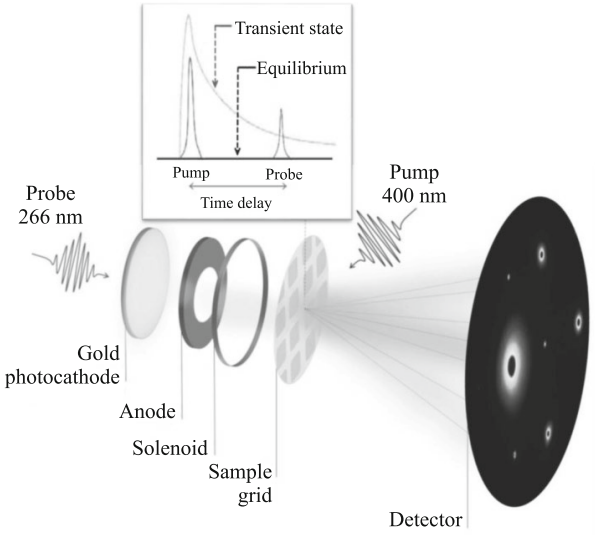

Fig. 1. Sketch of the ultrafast electron diffraction experimental setup. The electron bunch generated in the photocathode (the third harmonic of the femtosecond Ti:sapphire laser) is accelerated in the electric field and is focused by the solenoidal magnetic lens. The sample was excited by the second harmonic of the same Ti:sapphire laser. The diffraction pattern was recorded by the position-sensitive detector.

The thin gold film was used in [7–12, 14] in the linear photoelectric effect regime, but two-photon electron emission in such a cathode irradiated by laser pulses in the visible band opens new possibilities. An example is the compact femtosecond electronograph described in [13], where femtosecond laser radiation ($\lambda \cong 565$ nm, $\hbar\omega \cong 2.2$ eV) at the output of a parametric amplifier was used. Tuning the wavelength to the two-photon emission threshold, the authors achieved high coherence of the probe due to zero initial kinetic energy of electrons. This enabled the detection of deviations [13, 15] from the well-known two-temperature model describing the dynamics of the excitation of the electron and phonon subsystems in solids [16, 17]. A stable source of single electron pulses (for which the effective work function W_{Au} was about 4.3 eV), where the Coulomb repulsion was almost eliminated, was developed on the basis of two-photon electron emission [18, 19].

3. FACTORS AFFECTING THE WORK FUNCTION OF THE GOLD CATHODE

To reveal reasons why the threshold 4.3–4.4 eV of photoelectron emission from the thin gold film [13, 18, 19] appears to be noticeably lower than the reported data 5.1–5.3 eV [20–22]), we consider several factors. First, it is known from the description of Schottky effect [21] that an external electric field F reduces the work function W. If the surface of the planar cathode is uniform, this decrease ΔW measured in

electronvolts in the applied electric field strength F measured in volts per centimeter is

$$\Delta W \cong 3.8\times10^{-4}\sqrt{F}. \quad (1)$$

A high field strength F should be maintained in the accelerating gap of the electronograph because the acceleration of electrons in a short segment makes it possible not only to minimize the time of flight to the sample but also to reduce the effect of the spread in the initial energies of electrons to reach a high time resolution. However, to prevent breakdowns and to ensure the stable operation of the device, the maximum field strength F is limited at a level of 10^5 V/cm. Then, according to Eq. (1), $\Delta W \cong 0.1$ eV, which cannot explain the above discrepancy. Other reasons for it should be considered.

As mentioned in [23], a significant decrease in W_{Au} from ≈5.1 to ≈4.4 eV can be due to chemisorption of a tightly bound monolayer of polar molecules (such as water) and hydrocarbons. The authors of [24] studied the dynamics of the surface pollution of Au(111) grown on silica substrates at different times (minutes, hours, days) by scanning atomic force microscopy and Kelvin probe force microscopy, which provided the understanding of surface rearrangement mechanisms responsible for the variation of W_{Au} between 5.25 and 4.75 eV exclusively due to different storage conditions of the gold sample, e.g., in open air and in a hermetically closed container in the same laboratory. The so-called advective carbon (AdC) appeared to present everywhere on the surface of almost all inorganic materials due to the airborne mechanism. Two pollution regimes were revealed in [24]. The initial fast phase corresponds to the adsorption of organic molecules on the gold surface during several minutes after changes in the environmental conditions. The accumulation of AdC in the slower phase is accompanied by the migration of carbon-containing clusters over the surface and by their growth.

On the one hand, the organic film on the surface of the gold cathode can explain the possibility of electron emission under the action of laser pulses in the ultraviolet band ($\hbar\omega \cong 4.65$–4.75 eV) in the linear photoelectric effect regime. However, on the other hand, the long-term stable operation of the source of electrons in high vacuum requires clean experimental conditions under which the AdC film can be easily destroyed by ultraviolet laser pulses. In this context, it is important to understand whether this description is complete and whether the mechanism of reducing the work function of gold due to the presence of carbon-containing molecules (or polar water molecules) on its surface is the only possible.

4. PHOTOELECTRON EMISSION MECHANISM IN THE Cr/Au BIMETALLIC STRUCTURE UNDER THE ACTION OF FEMTOSECOND LASER PULSES

We take into account that a compact photoelectron source for many UED schemes is a bimetallic nanostructure. In [7–13], the emitting gold layer was deposited on a special buffer layer to increase the adhesion of Au to the transparent substrate through which ultraviolet radiation was delivered to the cathode in vacuum (see Fig. 2). In particular, the thin-film gold photocathode on a sapphire substrate for the experimental setup in [11] was prepared by electron beam evaporation when the 1-nm-thick adhesive Cr layer was first deposited and it was then coated by the 20-nm-thick Au layer.

We emphasize the following important circumstance. According to the precise measurements of the quantum efficiency of photoelectron emission in [13, 18, 19], the work function of the thin-film cathode is about 4.3–4.4 eV, which coincides with W_{Cr}. Indeed, chromium has a comparatively low work function of ≈4.4 eV, which, together with the developed method of uniform growth of thin films, ensures its numerous applications [25].

The properties of bimetallic structures such as Cr/Au are of particular interest. Using electron microscopy, atomic force microscopy, and X-ray photoelectron spectroscopy, the authors of [26] studied in detail the effect of the adhesive Cr layer on the structure of 2–20-nm-thick Au films. It was found that the predominant crystalline orientation of gold in all samples was [111], and the chromium layer was partially oxidized [26].

Taking into account that the oxide film can prevent the electric contact between Cr and Au, we use the electron energy diagrams for two isolated Au and Cr metallic layers. In this (Cr–oxide layer–Au) sandwich model, conduction electrons tunnel (see Fig. 3a) from the Cr film to the Au bulk through the oxide layer

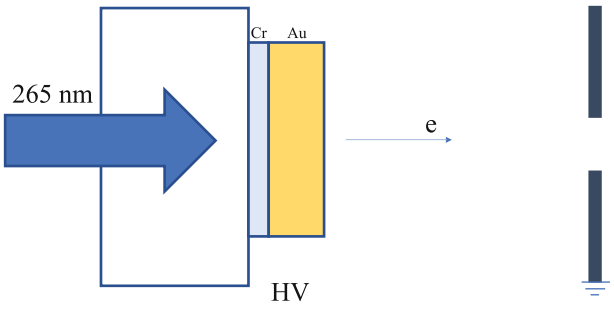

Fig. 2. (Color online) Thin-film Cr/Au structure under the action of transmitting ultraviolet laser radiation emits electrons, which are then accelerated by the static electric field in the gap between the cathode to which a high negative voltage HV is applied and the anode.

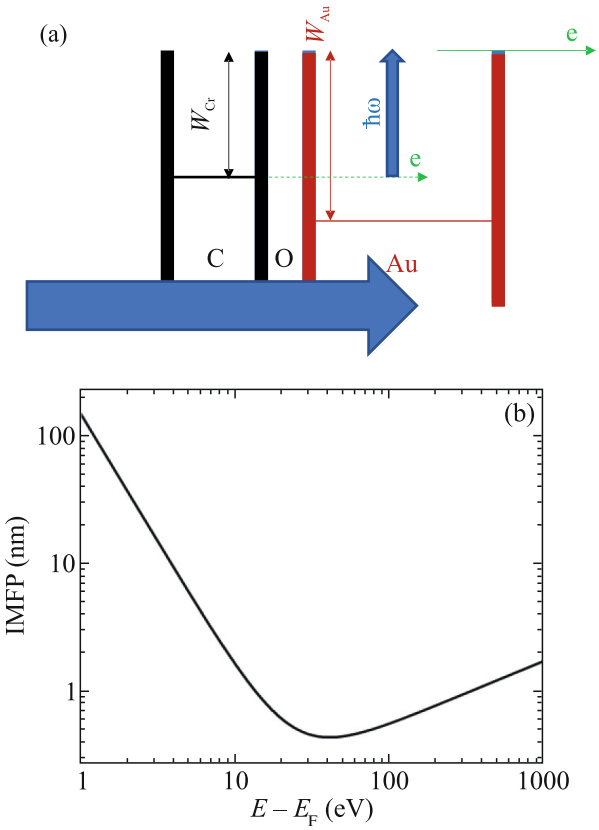

Fig. 3. (Color online) (a) Illustration of the (Cr–oxide layer–Au) sandwich model for the observation of the photoelectron emission. It is taken into account that the oxide film O is formed on the Cr layer in the process of fabrication of the thin-film gold cathode and can prevent the electric contact between Cr and Au. (b) Universal curve qualitatively representing the dependence of the inelastic free path of electrons in a solid on the kinetic energy of electrons [27]. The electron inelastic mean free paths in gold calculated in [28] are summarized in Table 1.

(CrO_x, $1 < x < 1.5$) whose conductivity can "shortly appear" under the action of ultraviolet laser pulses (or intense pulses in the visible band). Electrons with the energy $W_{Au} - W_{Cr} \approx 1$ eV can propagate "ballistically" in the gold film to a length of several tens of nanometers (see Fig. 3b), which is in fact equal to the cathode thickness. The threshold of photoelectron emission for these electrons is ≈4.4 eV, which is in good agreement with the experiment [13, 18, 19].

In this model, the role of the gold film as an inert layer is in fact reduced to the maintenance of the unchanged structure of the sandwich itself. To use a comparatively thick protective gold film (Au thickness of 20–30 nm), the difference between the work function of the buffer layer and W_{Au} should be not too large because the electron inelastic mean free path in gold decreases sharply with increasing kinetic energy (see the left part of Fig. 3b and Table 1). The electron inelastic mean free path in Fig. 3b is described by the function [27]

$$\text{IMFP} = 143/(E - E_F)^2 + 0.054\sqrt{(E - E_F)}, \qquad (2)$$

where E_F is the Fermi energy, the electron inelastic mean free path IMFP is measured in nanometers, and the energy difference $E - E_F$ is measured in electronvolts. Since Eq. (2) is applicable only for a qualitative description, electron inelastic mean free paths for gold calculated according to [28] are summarized in Table 1.

Table 1. Electron inelastic mean free path IMFP in gold according to [28]

$E - E_F$ (eV)	1	2	3	4
IMFP (nm)	30–40	10–20	5–7	3–4

An unconventional character of the multiphoton generation of electrons in a bimetallic structure was previously detected in [29], where gold films with different thicknesses on an aluminum substrate were irradiated by femtosecond laser pulses ($\lambda \cong 780$ nm, $\hbar\omega \cong 1.6$ eV). It was established that the four-photon emission (characteristic of $W_{Au} \cong 5.3$ eV) at the P polarization and the layer thickness ≈43 nm was replaced by the three-photon process; this behavior was attributed to the anomalous photoelectric effect in gold at the femtosecond scale. Taking into account that the total energy of three photons is ≈4.8 eV, this result [29] indicated a significant decrease in the threshold of electron emission from the metal. The numerical simulation in [30] for the Al/Au metallic structure shows that the field gradient of exited surface plasmons reached a maximum at the interface, which ensured a significant acceleration of electrons due to the ponderomotive force induced by femtosecond radiation. Thus, the metallic substrate can significantly affect the photoelectric effect in the gold film.

According to the model we proposed, the threshold of photoelectron emission from the bimetallic photocathode (with the outer gold protective layer) is determined by the work function of the metallic buffer W. This opens the potential possibility of controlling the initial energy distribution of emitted electrons by selecting the buffer, which can be used to increase the coherence of the probe beam in the UED method (when the work function W coincides with the photon energy of one of the harmonics of the femtosecond laser). In particular, the use of yttrium with the work function $W_Y \cong 3$ eV to fabricate the Au/Y bimetallic structure will possibly allow one to use the second harmonic of the Ti:sapphire laser ($\lambda = 400$ nm, $\hbar\omega \cong 3.1$ eV) not only to form electron pulses with almost zero initial energy but also to correspondingly simplify the detection scheme for the structural dynamics on a compact device.

5. CONCLUSIONS

It is noteworthy that only copper and silver, which have (according to the reference data) a comparatively low work functions: $W_{Cu} \cong 4.4$ eV and $W_{Ag} \cong 4.3$ eV for polycrystals, are mentioned as materials for photocathodes in review [1] of studies concerning the ultrafast electron diffraction method. At the same time, compact sources of electrons based on the thin-film gold cathode made it possible to carry out a number of corresponding successful experiments [7–14], involving the subthreshold ultrafast photoelectron emission process.

"The gold photocathode problem" is the most pronounced in the linear photoelectric effect, when the ultrafast heating of the ensemble of free electrons and, correspondingly, a significant (by ≈1 eV) decrease in W_{Au} can be excluded due to the tail of the electron Fermi distribution. Indeed, in contrast to the two-photon process, laser pulses used for the linear photoelectric effect had a comparatively low intensity, which ensured the long-term stable operation of the photoelectron source.

Just the carbon-containing film on the Au surface possibly ensures an anomalously low work function for photoelectron emission.

In the model we proposed, where it is taken into account that the oxide film is formed on the Cr layer in the process of fabrication of the Au/Cr bimetallic gold cathode and prevents the electric contact between Cr and Au, only the thin chromium layer is involved in the emission, whereas the role of the gold film as an inert layer is reduced to the maintenance of the unchanged structure of the (Cr–oxide layer–Au) sandwich. Here, electrons from the Fermi level in chromium tunnel to the gold bulk (it seems important to take into account the possibility of the fast appearance of the conductivity of the oxide layer under the action of femtosecond laser pulses). Electrons propagate ballistically over the entire thickness of the gold film, where they acquire the energy necessary for photoelectron emission. Using the reference work functions for Cr and Au, we have achieved good agreement with experiment.

ACKNOWLEDGMENTS

We are grateful to A.A. Sokolik and Yu.E. Lozovik for careful reading of the manuscript and valuable remarks.

FUNDING

This work was supported by the Ministry of Science and Higher Education of the Russian Federation (state assignment FFUU-2022-0004 for the Institute of Spectroscopy, Russian Academy of Sciences).

CONFLICT OF INTEREST

The authors of this work declare that they have no conflicts of interest.

REFERENCES

1. D. Filippetto, P. Musumeci, R. K. Li, B. J. Siwick, M. R. Otto, M. Centurion, and J. P. F. Nunes, Rev. Mod. Phys. **94**, 045004 (2022).
2. A. De La Torre, D. M. Kennes, M. Claassen, S. Gerber, J. W. McIver, and M. A. Sentef, Rev. Mod. Phys. **93**, 041002 (2021).
3. A. A. Ishchenko, G. V. Fetisov, and S. A. Aseyev, *Methods for Detecting Ultrafast Dynamics of Matter* (Fizmatlit, Moscow, 2022) [in Russian].
4. S. A. Aseyev, A. S. Akhmanov, G. V. Girichev, A. A. Ishchenko, I. V. Kochikov, V. Ya. Panchenko, and E. A. Ryabov, Phys. Usp. **63**, 103 (2020).
5. Ch. Li, M. Guan, H. Hong, K. Chen, X. Wang, H. Ma, A. Wang, Zh. Li, H. Hu, J. Xiao, J. Dai, X. Wan, K. Liu, Sh. Meng, and Q. Dai, Sci. Adv. **9**, eadf4170 (2023).
6. C. Hong, W. Zou, P. Ran, K. Tanaka, M. Matzelle, W. C. Chiu, R. S. Markiewicz, B. Barbiellini, Ch. Zheng, S. Li, A. Bansil, and R. H. He, Nature (London, U.K.) **617**, 493 (2023).
7. I. G. Vallejo, G. Gallé, B. Arnaud, S. A. Scott, M. G. Lagally, D. Boschetto, P. E. Coulon, G. Rizza, F. Houdellier, D. Bolloc'h, and J. Faure, Phys. Rev. B **97**, 054302 (2018).
8. Y. Morimoto, R. Kanya, and K. Yamanouchi, J. Chem. Phys. **140**, 064201 (2014).
9. M. S. Robinson, P. D. Lane, and D. A. Wann, Rev. Sci. Instrum. **86**, 013109 (2015).
10. C. J. Hensley, J. Yang, and M. Centurion, Phys. Rev. Lett. **109**, 133202 (2012).
11. A. Zong, Doctoral Thesis (Massachusetts Inst. Technol., MA, USA, 2021).
12. A. Zong, Q. Zhang, F. Zhou, et al., Nature (London, U.K.) **620**, 988 (2023).
13. L. Waldecker, R. Bertoni, and R. Ernstorfer, J. Appl. Phys. **117**, 044903 (2015).

14. S. A. Aseyev, E. A. Ryabov, B. N. Mironov, I. V. Kochikov, and A. A. Ischenko, Chem. Phys. Lett. **797**, 139599 (2022).
15. L. Waldecker, R. Bertoni, R. Ernstorfer, and J. Vorberger, Phys. Rev. X **6**, 021003 (2016).
16. S. I. Anisimov, A. M. Bonch-Bruevich, M. A. El'yashevich, Ya. A. Imas, N. A. Pavlenko, and G. S. Romanov, Sov. Phys. Tech. Phys. **11**, 945 (1967).
17. S. I. Anisimov, B. L. Kapeliovich, and T. L. Perel'man, Sov. Phys. JETP **66**, 776 (1974).
18. M. Aidelsburger, F. O. Kirchner, F. Krausz, and P. Baum, Proc. Natl. Acad. Sci. **107**, 19714 (2010).
19. L. Kasmi, D. Kreier, M. Bradler, E. Riedle, and P. Baum, New J. Phys. **17**, 033008 (2015).
20. W. M. H. Sachtler, G. J. H. Dorgelo, and A. A. Holscher, Surf. Sci. **5**, 221 (1966).
21. *Handbook of Physical Quantities,* Ed. by I. S. Grigoriev and E. Z. Meilikhov (Energoatomizdat, Moscow, 1991; CRC, Boca Raton, NY, 1996).
22. *CRC Handbook of Chemistry and Physics,* 95th ed., Ed. by W. M. Haynes, D. R. Lide, and T. J. Bruno (CRC, Taylor and Francis Group, Boca Raton, 2014).
23. P. J. Wass, D. Hollington, T. J. Sumner, F. Yang, and M. Pfeil, Rev. Sci. Instrum. **90**, 064501 (2019).
24. N. Turetta, F. Sedona, A. Liscio, M. Sambi, and P. Samori, Adv. Mater. Interfaces **8**, 2100068 (2021).
25. A. Moradi, M. Rog, G. Stam, R. M. Tromp, and S. J. van der Molen, Ultramicroscopy **253**, 113809 (2023).
26. M. Todeschini, A. Bastos da Silva Fanta, F. Jensen, J. B. Wagner, and A. Han, ACS Appl. Mater. Interfaces **9**, 37374 (2017).
27. M. P. Seah, W. A. Dench, Surf. Interface Anal. **1**, 2 (1979).
28. H. T. Nguyen-Truong, J. Phys. Chem. **119**, 7883 (2015).
29. J. Kupersztych and M. Raynaud, Phys. Rev. Lett. **95**, 147401 (2005).
30. M. Raynaud and J. Kupersztych, Phys. Rev. B **76**, 241402(R) (2007).

Translated by R. Tyapaev